Journal of ELECTRONIC MATERIALS, Vol. 47, No. 8, 2018
https://doi.org/10.1007/s11664-018-6294-6
© 2018 The Minerals, Metals & Materials Society

CrossMark

TOPICAL COLLECTION: 18TH INTERNATIONAL CONFERENCE ON II-VI COMPOUNDS

Effects of Nitrogen Partial Pressure Ratio and Anneal Temperature on the Properties of Al–N Co-Doped ZnO Thin Films

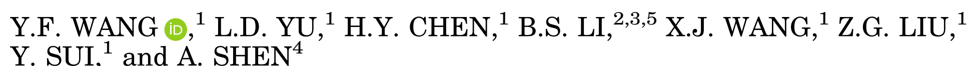

Y.F. WANG,[1] L.D. YU,[1] H.Y. CHEN,[1] B.S. LI,[2,3,5] X.J. WANG,[1] Z.G. LIU,[1] Y. SUI,[1] and A. SHEN[4]

1.—Department of Physics, Harbin Institute of Technology (HIT), Harbin 150080, China. 2.—State Key Laboratory of Urban Water Resource and Environment, Department of Physics, Harbin Institute of Technology, Harbin, China. 3.—Key Laboratory for Photonic and Electronic Bandgap Materials, Ministry of Education, Harbin Normal University, Harbin, China. 4.—Department of Electrical Engineering, The City College of New York, New York 10031, USA. 5.—e-mail: libingsheng@hit.edu.cn

The authors report the conversion of conduction type from *n*-type to *p*-type in the Al–N co-doped ZnO thin films by using thermal annealing treatment under argon atmosphere. The samples were deposited on fused silica by radio frequency magnetron sputtering. X-ray diffraction measurements showed that ZnO thin films have (002)-preferred orientation and the lattice constant decreases with the increase of nitrogen partial pressure. The average optical transmittance of these films is over 80%. The hole density is around 1.58×10^{17} cm^{-3} with an annealing temperature of 700°C. After exposing the samples in air for 1 year, the conduction type remains *p*-type with only a slight decrease of hole density, which indicates that the *p*-type ZnO with Al–N co-dopants has good electrical stability.

Key words: *p*-type ZnO, Al–N co-doping, annealing, RF magnetron sputtering

INTRODUCTION

As a direct wide band gap semiconductor with a large exciton binding energy of 60 meV, zinc oxide (ZnO) has been recognized as a promising material for ultraviolet (UV) light-emitting diodes (LEDs) and laser diodes (LDs).[1–4] To realize these applications, an important issue is the fabrication of high-quality *n*-type and *p*-type ZnO material with low resistance. ZnO is naturally an *n*-type wide band gap semiconductor.[5] However, it is difficult to obtain efficient *p*-type doping due to the strong self-compensation effect.[6] In order to realize *p*-type doping in ZnO, a variety of elements have been selected as acceptors to substitute the Zn or O, including group I (Li, Na, K, Cu, Ag) and group V (N, P, As, Sb) elements.[7–12] Among those elements, N has been demonstrated as a good *p*-type dopant for ZnO because its ionic radius is close to O as well as the success of *p*-type doping in II–IV selenides with N dopant.[13] Much literature on the growth of *p*-type ZnO is available. However, it is still difficult to obtain *p*-type ZnO, which has been attributed to the self-compensation by native defects and the low solubility of N in ZnO due to its high formation energy. To improve the acceptor solubility, a co-doping method using group V acceptors and group III reactive donors has also been proposed to create *p*-type conduction.[14–16] The calculations suggest that co-doping can decrease the ionized energy of the acceptor and sufficiently increase dopant solubility due to the low formation enthalpy. The theory was later proved by experiments. Therefore, co-doping with group IIIA and V elements may be a promising way to realize *p*-type ZnO.

In previous work, we reported an alternative route of thermal oxidization of Zn_3N_2 to prepare *p*-type ZnO

(Received December 25, 2017; accepted April 10, 2018; published online April 25, 2018)
Y.F. Wang and L.D. Yu have contributed equally to his work.

thin films.[17] *p*-type ZnO:N with a hole density of 4.16×10^{17} cm^{-3} has been obtained at an optimized annealing temperature of 700°C. Recently, we improve the thermal stability of *p*-type ZnO by thermal oxidization of Al-doped Zn_3N_2.[18] Due to the strong chemical bond of Al–N, the Al can stabilize the N and avoid the over replacement of residual N by O during the annealing at high temperature. However, as pointed out in a recent paper about the limitation of ZnN oxidation, abundant defects remain and could not be completely eliminated by annealing treatment.[19] In order to overcome this limitation and improve the structural quality of ZnO thin films, we prepare Al–N co-doped ZnO using a co-sputtering method with the introduction of ZnO and AlN ceramic targets. In this paper, we systematically study the effects of nitrogen-to-argon ratio and thermal annealing on structural, optical and electrical properties of ZnO. X-ray diffraction (XRD) indicated that all samples are (002)-preferred oriented. After annealing treatment in oxygen atmosphere, *p*-type ZnO samples with high stability have been obtained.

EXPERIMENTAL PROCEDURES

The Al–N co-doped ZnO thin films were deposited on fused silica glass substrates by radio frequency (RF) magnetron sputtering. The substrates were cleaned with ethanol and acetone in an ultrasonic bath for 10 min and then rinsed with deionized water. The substrates were dried by nitrogen gas before being fixed to a rotating substrate holder. ZnO (purity of 99.99%) and AlN (purity of 99.99%) materials were selected as the co-sputtering targets. The base pressure and working pressure were 5×10^{-4} Pa and 3.0 Pa, respectively. During the deposition, the RF power of ZnO and AlN targets was fixed at 150 W and the films were deposited for 30 min. The ratio of nitrogen (N_2) and argon (Ar) flow was set at 0:25, 5:20, 10:15, 15:10 and 20:5 sccm. Subsequently, the films prepared at different nitrogen partial pressures were annealed at 500°C, 600°C, 700°C, and 800°C in a tube furnace under argon atmosphere for 60 min.

To investigate the properties of the co-doped films, XRD analysis (source Cu Kα with λ = 1.54 Å) was performed to obtain the structural parameters and to study the possible phases of the fabricated films. Scanning electron microscopy (SEM) was used to investigate the surface morphology of the co-doped thin films. Energy-dispersive x-ray spectroscopy (EDS) was used to identify the elements present in the films. The optical characteristics were measured by an UV–visible spectrophotometer. The electrical properties of the films were measured using van der Pauw Hall measurement (HL5500PC) at room temperature.

RESULTS AND DISCUSSION

Structure and Morphology Properties

Figure 1 is the XRD pattern of the Al–N co-doped ZnO prepared at different nitrogen partial pressure ratios. It is obvious that only a (002) diffraction peak is observed in all films which is indexed as the hexagonal wurtzite crystal structure of ZnO. No Al_2O_3 and Zn_3N_2 phases were found implying that the Al and N atoms occupied the former sites of Zn and O. In addition, the diffraction angle of the (002) peak shifted to a higher angle and the full width at half maximum (FWHM) decreased as the nitrogen partial pressure was increased. Table I lists the structure parameters of the co-doped films calculated from the XRD spectra. The crystalline plane distance (d) was calculated by the Bragg diffraction equation: $\lambda = 2d\sin\theta$. The average crystallite dimension of the Al–N codoped thin films calculated from the FWHM is about 16–24 nm according to the Scherrer formula. From Table I, we found that the 2θ value of the (002) peak for all co-doped films is smaller than that of bulk ZnO (34.40°). According to solid solution principle, Al-doped ZnO would lead to a larger 2θ value and N-doped ZnO to a smaller value. In addition, the existence of residual stress in the films also contributes to the shift in diffraction angle. There are several reasons for the existence of stress, such as lattice mismatch, deposition under non-equilibrium conditions as well as the dopant and composition gradient across the film surface. Since the length of the Zn–N bond is slightly shorter than that of the Zn–O bond, the change in lattice constant would be attributed to the substitution of N atoms for O atoms.

Optical Analysis

Figure 2 shows the optical transmission and absorption spectra of Al–N co-doped ZnO thin films prepared at different nitrogen partial pressure ratios. The thickness of these films is about 450 nm as determined by the step profiler. As we can see, the fluctuation in the visible region is caused by the interference of light. The average optical transmittance of these films is over 80%. For the sample prepared at a nitrogen partial pressure

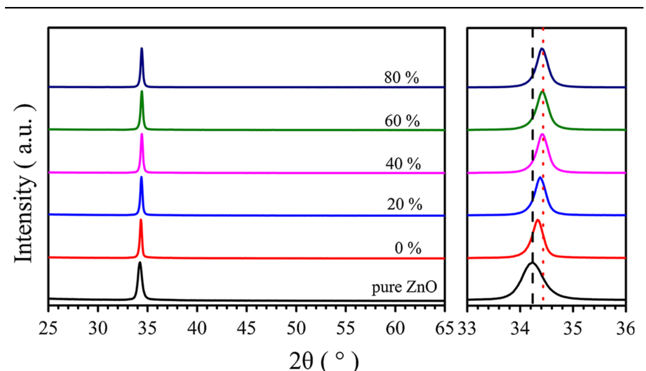

Fig. 1. XRD patterns of Al–N co-doped ZnO thin films prepared at different nitrogen partial pressure ratios. All films show (002)-preferred orientation (left). The diffraction peaks shift to a high angle with the introduction of N_2 as well as the increase of N_2 partial pressure ratio (right).

Table I. Structural parameters of Al–N co-doped ZnO thin films prepared at different nitrogen partial pressure ratios, including diffraction angle (2*θ*), full width at half maximum (FWHM), interplanar distance (*d*), and lattice constant (*c*)

Samples	2*θ* (°)	FWHM (°)	*d* (Å)	*c* (Å)
Pure ZnO	34.213	0.452	2.6187	5.2374
0%	34.293	0.257	2.6127	5.2254
20%	34.345	0.258	2.6089	5.2178
40%	34.396	0.266	2.6052	5.2104
60%	34.396	0.276	2.6052	5.2104
80%	34.372	0.266	2.6069	5.2138

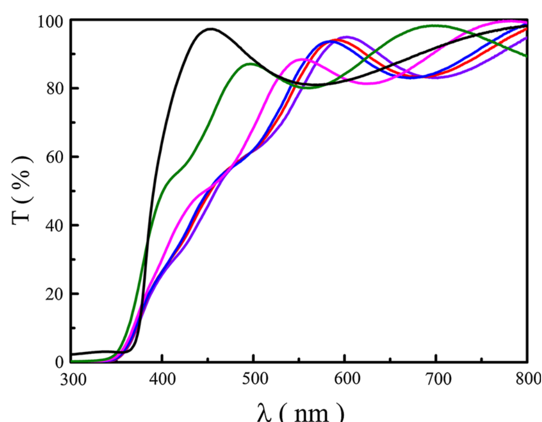

Fig. 2. Optical transmission spectra of the Al–N co-doped ZnO thin films prepared at different nitrogen partial pressure ratios.

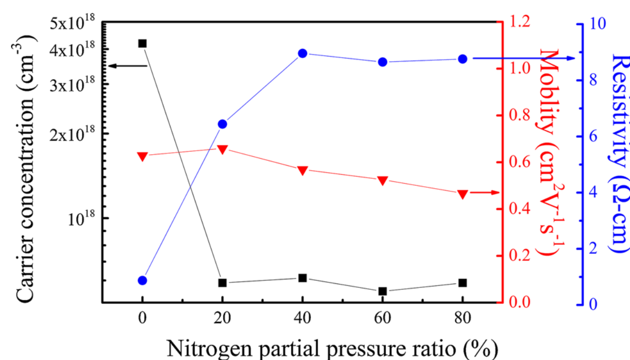

Fig. 3. Effect of nitrogen partial pressure ratio on the electrical properties of Al–N co-doped ZnO thin films. The square is the carrier concentration. The triangle is the Hall mobility. The circle is the resistivity.

of 0:25 (without nitrogen), the sharp absorption edge and high optical transmittance in the visible region were observed. On the contrary, the absorption edge of Al–N co-doped ZnO thin films deposited under different nitrogen atmospheres shifted to a longer wavelength. This is ascribed to the large number of deep-level defects formed by the introduction of N_2.

Electrical Properties

The effect of nitrogen partial pressure ratio on the resistivity, carrier concentration and mobility are shown in Fig. 3. All the films were in a square shape of 1×1 cm^2. Indium was used as electrode material and all samples showed good Ohmic contact. The Hall results show that the co-doped thin films are *n*-type conductivity. It is known that the substitutional Al atoms form shallow donors and contribute conduction electrons. During sputtering, N_2 was decomposed into nitrogen atoms and/or nitrogen ions. Either nitrogen atoms or nitrogen ions are very active. They can fill the oxygen vacancy and combine with Al atoms. Compared with the films prepared in pure argon atmosphere, the carrier concentration of co-doped ZnO thin films fabricated at different nitrogen partial pressures show obvious decrease, indicating that the N atoms are effectively

Table II. Electrical measurement results of Al–N co-doped ZnO thin films prepared at different nitrogen partial pressure ratios measured with an HL5500PC system

Sample	Carrier concentration (cm^{-3})	Hall mobility (cm^2/V s)	Sheet resistance (Ω/sq)	Resistivity (Ω·cm^2)	Carrier type
0%	4.19×10^{18}	0.63	23,700	0.87	*n*
20%	5.88×10^{17}	0.66	161,000	6.44	*n*
40%	6.12×10^{17}	0.57	179,200	8.96	*n*
60%	5.49×10^{17}	0.53	216,200	8.65	*n*
80%	5.88×10^{17}	0.47	227,500	8.76	*n*

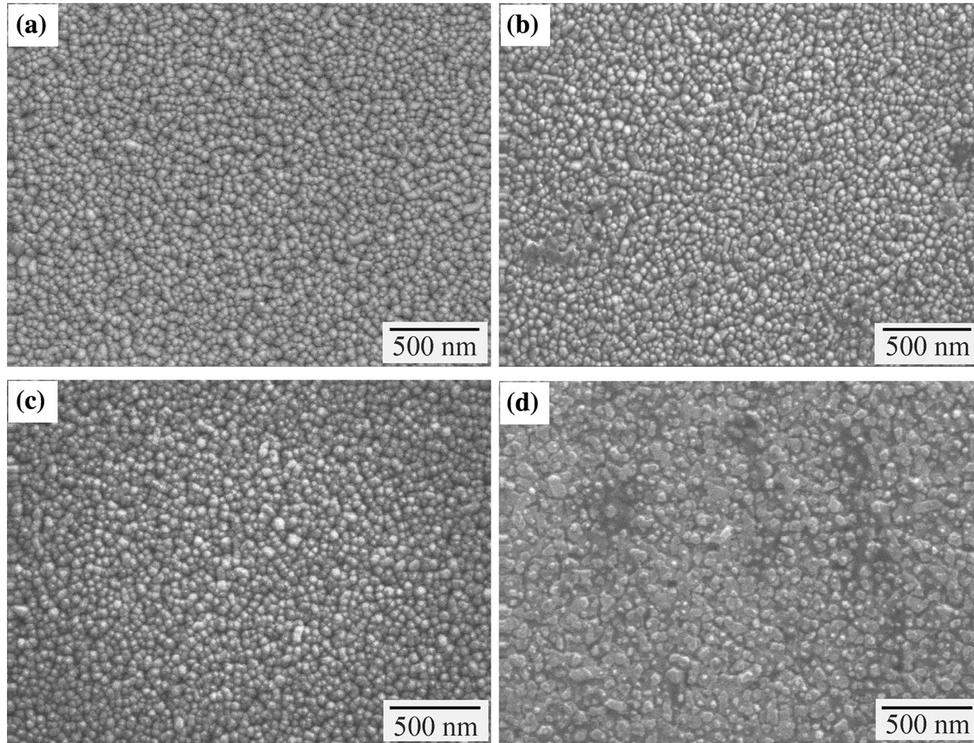

Fig. 4. SEM images of Al–N co-doped ZnO thin films annealed at (a) 500°C, (b) 600°C, (c) 700°C, and (d) 800°C. The crystalline quality of the samples is improved by raising the annealing temperature, and the crystal grain size is increased.

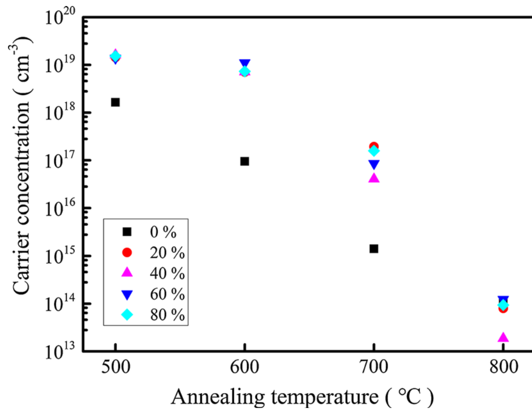

Fig. 5. Effect of thermal annealing temperature on the conduction type and carrier concentration of Al–N co-doped ZnO thin films. The carrier concentration decreases with the increase of annealing temperature. The films prepared under different nitrogen partial pressure ratios convert to *p*-type at the temperature over 700°C (upper) while the film deposited under pure argon atmosphere still shows *n*-type (lower). The films prepared under pure argon atmosphere show *n*-type at any temperatures.

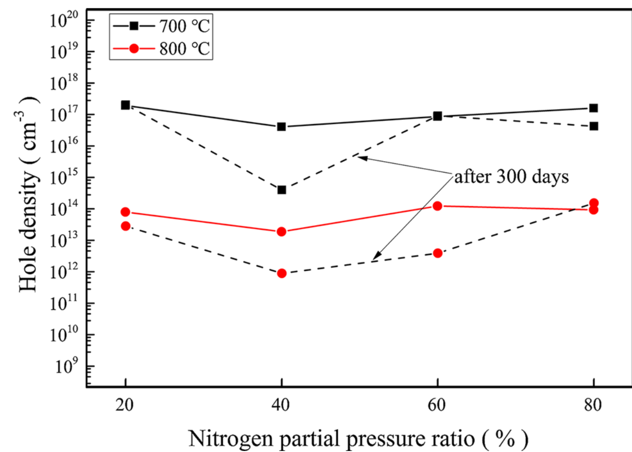

Fig. 6. The change of hole density after exposure in air for 300 days.

doped into ZnO films. Table II lists the details of the electrical parameters. It can be found that the electron concentration decreased from 4.19×10^{18} cm^{-3} to 5.88×10^{17} cm^{-3} and the resistivity increased from 0.87 to 6.44 $\Omega \cdot cm^2$ as the nitrogen was introduced. However, the nitrogen partial pressure in this work did not make much different in the electrical property of Al–N co-doped ZnO films probably due to the limited solubility of N in the material.

Thermal Annealing Influence

In order to activate the N-related acceptors to realize *p*-type conductivity, the films prepared at different nitrogen partial pressure ratios were annealed in a tube furnace at 500°C, 600°C, 700°C, and 800°C for 60 min under argon atmosphere. As a comparison, the Al–N co-doped ZnO

thin films prepared without nitrogen were also annealed. XRD structural analysis showed that these annealed Al–N co-doped ZnO films all have preferred (002) orientation, similar to those of the unannealed samples. Figure 4 is the SEM images of co-doped ZnO films annealed at different temperatures. Results show that the grain size and the compactness increased with increase of temperature. Figure 5 is the electrical properties of co-doped ZnO films annealed at different temperatures. With the increase of annealing temperature, the carrier concentration gradually decreased, indicating that the N-related acceptors were effectively activated. When the annealing temperature reached 700°C, the annealed Al–N co-doped ZnO films had the highest hole concentration of 1.582×10^{17} cm^{-3}, resistivity of 80.12 Ω·cm^2 and Hall mobility of 0.492 cm^2 V^{-1} s^{-1}. By further increasing the annealing temperature, more donor-related defects were generated. Beside this, the N atoms easily formed N_2 to escape to the atmosphere at high annealing temperatures. All these factors contribute to the decrease of hole density. It is worth noting that the films prepared under pure argon atmosphere show *n*-type at any temperatures, indicating that the existence of N_2 is the key factor in the preparation of *p*-type Al–N co-doped ZnO. To investigate the stability of the films, each *p*-type thin film was measured after exposure in air for 300 days. Figure 6 shows how the hole density changes over 300 days. The results indicate that the *p*-type characteristics of the co-doped ZnO thin films were still well maintained with only a slight decrease in hole concentration due to the stabilization of N acceptors with Al–N bonding.[18]

CONCLUSIONS

In summary, Al–N co-doped ZnO thin films were deposited by RF magnetron sputtering at different nitrogen partial pressure ratios. All films showed preferred (002) orientation with *n*-type conductivity. The *p*-type Al–N co-doped ZnO with a maximum hole density of 1.58×10^{17} cm^{-3} was obtained at annealing temperatures over 700°C. They still show *p*-type characteristics after exposure in air for 300 days with only a slightly decrease in hole density, indicating good stability. Deposition of intrinsic *n*-type ZnO onto our *p*-type ZnO films will make it possible to produce a a *p*–*n* junction diode.

ACKNOWLEDGEMENTS

This work was supported by the National Natural Science Foundation of China (11474076), the Post-doctoral Science-Research Developmental Foundation of Heilongjiang Province (Grant No. LBH-Q13082), Open Project of State Key Laboratory of Urban Water Resources and Water Environment, Harbin Institute of Technology (No. ES201702) and Open Project of Key Laboratory for Photonic and Electronic Bandgap Materials, Ministry of Education, Harbin Normal University (PEBM201506).

REFERENCES

1. Ü Özgür, Ya I Alivov, C Liu, A Teke, MA Reshchikov, S Doğan, V Avrutin, SJ Cho, and H Morkoçl, *J. Appl. Phys.* 98, 11 (2005).
2. YK Mishra, G Modi, V Cretu, V Postica, O Lupan, T Reimer, I Paulowicz, V Hrkac, W Benecke, L Kienle, R Adelung, and ACS Appl, *Mater. Inter.* 7, 14303 (2015).
3. YK Mishra, R Adelung, C Röhl, D Shukla, F Spors, and V Tiwari, *Antivir. Res.* 92, 305 (2011).
4. D Gedamu, I Paulowicz, S Kaps, O Lupan, S Wille, G Haidarschin, YK Mishra, and R Adelung, *Adv. Mater.* 26, 1541 (2014).
5. LG Wang, A. Zunger. *Phys. Rev. Lett.* 90, 256401 (2003).
6. H Sun, SU Jen, SC Chen, SS Ye, and X Wang, *J. Phys. D Appl. Phys.* 50, 099501 (2017).
7. K Yim, J Lee, D Lee, M Lee, E Cho, HS Lee, HH Nahm, and S Han, *Sci. Rep.* 7, 40907 (2017).
8. S Cho and IM Kang, *Adv. Mater.* 23, 4183 (2011).
9. HS Kang, BD Ahn, JH Kim, GH Kim, SH Lim, HW Chang, and SY Lee, *Appl. Phys. Lett.* 88, 202108 (2006).
10. EC Lee and KJ Chang, *Phys. Rev. B* 70, 115210 (2004).
11. CH Park, SB Zhang, and SH Wei, *Phys. Rev. B* 66, 073202 (2002).
12. DC Look, DC Reynolds, CW Litton, and RL Jones, *Appl. Phys. Lett.* 81, 1830 (2002).
13. RM Park, MB Troffer, CM Rouleau, and JM Depuydt, *Appl. Phys. Lett.* 57, 2127 (1990).
14. M Joseph, H Tabata, H Saeki, K Ueda, and T Kawai, *Phys. B* 302, 140 (2001).
15. T Yamamoto and H Katayamayoshida, *Jpn. J. Appl. Phys.* 38, 166 (1999).
16. M Joseph, H Tabata, and T Kawai, *Jpn. J. Appl. Phys.* 38, 1205 (1999).
17. BS Li, YC Liu, ZZ Zhi, DZ Shen, YM Lu, JY Zhang, XW Fan, RX Mu, and D Henderson, *J. Mater. Res.* 18, 8 (2003).
18. YF Wang, DY Song, L Li, BS Li, A Shen, and Y Sui, *Phys. Status Solidi C* 13, 585 (2016).
19. BS Li, ZY Xiao, JG Ma, and YC Liu, *Chinese. Phys. B* 26, 5 (2017).